

장주기구조물의 탄소성응답특성을 고려한 지진안전성 평가

방 명 석

충주대학교 안전공학과
(2011. 3. 19. 접수 / 2011. 6. 8. 채택)

Seismic Safety Assessment of Long Period Structures Base on Elastic/Inelastic Response Characteristics

Myung-Seok Bang

Department of Safety Engineering, Chungju National University
(Received March 19, 2011 / Accepted June 8, 2011)

Abstract : The earthquake characteristic assessment of social overhead facilities would be an important examination issue for seismic capacity enhancement. This study is intended to reasonably evaluate the structural behavior of long-period frame structures considering near-fault and far-fault earthquake characteristics. Elastic/inelastic time history analyses were performed by selecting the objective structure which can precisely reflect the effect of input ground motion. Based on the result of numerical analysis, we have investigated response aspects of shear force, moment, acceleration and displacement according to earthquake characteristics. Moreover, in order to understand the inelastic behavior of the objective structure, we have analyzed and compared collapse modes by considering the occurrence process of plastic hinges. The outcome of this research is expected to provide the basic information for the seismic safety assessment of long-period frame structures.

초 록 : 지진별 특성이 사회간접시설에 미치는 영향을 평가하는 것은 내진성능의 향상을 위해 중요한 검토사항이다. 이 연구에서는 근거리 및 원거리 지진의 특성을 고려하여 장주기 골조구조물의 구조거동을 합리적으로 평가하는 방법을 비교분석하였다. 이를 위해서 입력지진동의 영향을 명확하게 반영할 수 있는 대상구조물을 선정하여 탄성 및 비탄성 시간이력해석을 수행하였다. 수치해석결과를 바탕으로 지진특성에 따른 전단력, 모멘트, 가속도 및 변위응답의 분포양상을 검토하고 차이점을 분석하였다. 또한 대상구조물의 비탄성 거동을 파악하기 위해서 소성힌지의 발생순서를 모사운용하여 붕괴발생모드를 해석하였다. 이 연구결과는 장주기 골조구조물의 내진안전성 평가를 위한 효율적인 방법을 제시하고 근거리 지진의 안전성에 미치는 영향을 분석하였다.

Key Words : near fault earthquake, long period, frame structures, elastic/inelastic, time series, plastic hinge

1. Introduction

Near-fault earthquakes(NFE) occur around the area where there exist active fault zones, and seismic waves which near-fault earthquakes generate cause the disastrous results. This is why far-fault earthquakes(FFE) on which past seismic designs were based have different characteristics from those of near-fault earthquakes. With regard to fault actions, the most distinctive characteristic of near-fault earthquake is that the wave velocity with long periods in the beginning

stage of earthquake is high and ground is permanently displaced. Compared with normal far-fault earthquakes that has the same PGA (Peak Ground Acceleration), the energy of near-fault earthquakes is huge because their velocity and displacement are very large¹⁾. The studies on near-fault earthquakes started in the late 1950s, but at that time their importance was not known²⁾. Since the Northridge and Kobe earthquakes, however, it has been realized that near-fault earthquakes are not especial phenomena, and many studies have been published all over the world^{3,4)}. As for recent examples that evaluate the effect of near-fault earthquakes on facilities, there are few examples other

* To whom correspondence should be addressed.
msbang@cjnu.ac.kr

Table 1. Characteristics of selected input earthquake motions

Site	Station No.	D _{rup} * (km)	PGA (gal)		PGV (cm/s)**		PGV/PGA	
			EW	NS	EW	NS	EW	NS
Far-Fault Earthquakes	ILA002	109.11	47	71	10	11	0.21	0.15
	ILA035	104.77	69	51	11	10	0.16	0.20
Near-Fault Earthquakes	TCU052	1.84	349	439	183	221	0.53	0.50
	TCU068	3.01	495	358	280	292	0.57	0.81

* Distance from Rupture, ** PGV: Peak Ground Velocity

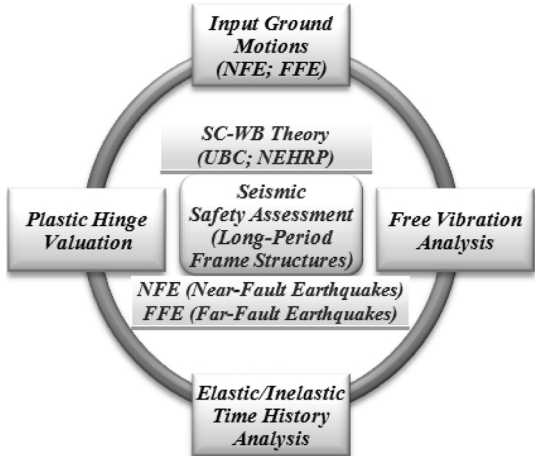


Fig. 1. Flow chart on seismic-safety evaluation of long-period frame structures.

than nuclear power plant⁵). In this study, the records of the Chi-Chi earthquake which Guo-Quan Wang corrected and distributed have been selected in order to consider earthquake characteristics⁶). Table 1 shows the locations of the measurement points of the Chi-Chi earthquake, the distance from the rupture and its characteristics, together with the PGA from the different directions. The effect of near-fault earthquakes on high-rise frame structures with long periods would be analyzed and compared to the effects of far-fault earthquakes based on the seismic response results by elastic/inelastic time history analyses. In addition, by investigating the formation process of plastic hinges, the inelastic response characteristics of selected earthquakes would be examined for the seismic safety enhancement of long-period frame structures. Fig. 1 illustrates the flowchart on seismic safety assessment of long-period frame structures which are implemented in this study.

2. Elastic/Inelastic Response Evaluation of Long-Period Frame Structures

2.1. Profile of the Objective Structure and Assumption Items

The inelastic behavior and damage of long-period frame structures are influenced by several factors, such as the stiffness of members, the number of occurrence of earthquakes, the frequency of ground motions, and the duration of strong base motion. Like the UBC or NEHRP, most of the seismic design standards recommend that structures have strong columns and weak beams (SC-WB), so that the structure should be able to disperse the incoming earthquake's motion well and induce ductile behavior.

In SC-WB structures, it is known that the displacement between adjacent floors is small, and the inelastic distortion appears all over the structure^{7,8}). Therefore, a 15-story, long-period frame structures was chosen as the objective structure of this study in Fig. 2. Then, based on the SC-WB theory, the elastic/inelastic behavior has been analyzed, according to the characteristics of the input earthquake motion. At that time, three assumptions for the long-period frame structure examined in this study are as follows. First,

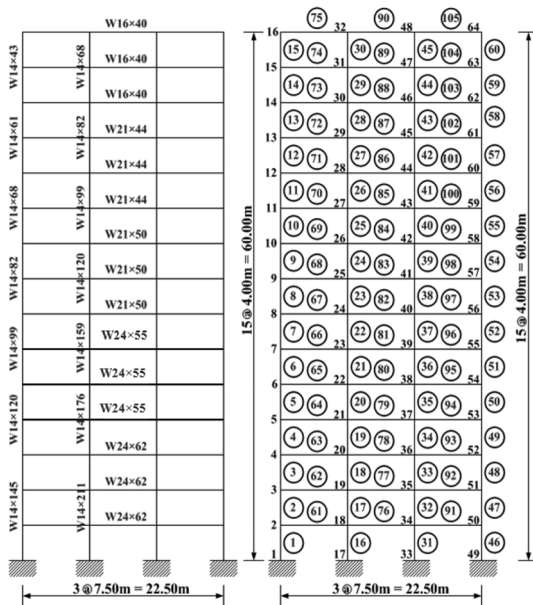


Fig. 2. Analytical modeling of the selected objective structure.

we assume that the structure is a rectangular-shaped, plane one with beams and columns, that the neutral axis of beams and columns is straight, and that their cross section does not change. In addition, it is assumed that the structure has been built based on SC-WB theory. The second assumption is concerned with the structural factor: the inelastic distortion by bending is focused on both ends of the beams, and it appears by plastic hinges. We also assume that the joints of beams and columns have bilinear behavior and beams and columns have shear distortion. The third assumption is about loads: the external load (including self-weight) applied to the members is a uniform load, and the ground moves only horizontally. For all mass in the dynamic analysis, lumped mass is used. Table 2 summarizes the characteristics of sections and members of the objective structure. Fig. 3 shows the yield criterion to reproduce the inelastic behavior of the structure. In the analytical modeling, we assume that the dead load of the structure on every floor is 40 kN/m, yield stress (f_y) is 2531 kPa, and strain hardening value 0.02.

2.2. Elastic/Inelastic Time History Analysis

The natural periods have been obtained by performing eigenvalue analysis of the objective structure. In order to verify the accuracy of this analysis, SAP 200N has been used, and then the results have been compared to those in this study. The natural periods of each mode are in agreement with those calculated to the third decimal point. It is evident that these values are accurate⁹⁾. Although up to 10th mode is shown in the Table 3, only the first five modes were

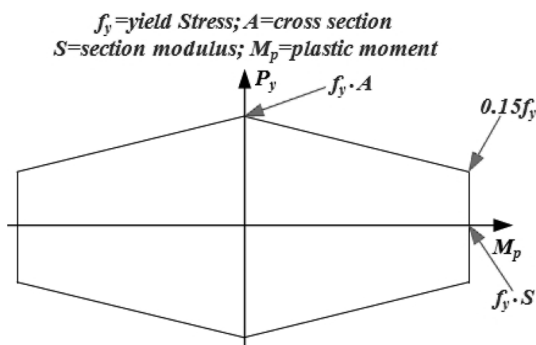


Fig. 3. Yield standards applied to the objective structure.

Table 2. Section and member properties of the objective structure

Member	Area, A(cm ²)	Moment of Inertia, I(cm ⁴)	Yield Load, P _y (kN)	Plastic Moment, M _p (kN-m)	
Column Elements	W14×43	81.2902	17814.71	2057.50	259.9113
	W14×61	115.4836	26638.81	2922.95	382.2168
	W14×68	129.0320	30093.53	3265.87	427.1724
	W14×82	155.4836	36711.61	3935.37	511.2826
	W14×99	187.7416	46201.69	4751.84	650.2671
	W14×120	227.7415	57439.94	5764.25	790.5741
	W14×145	275.4833	71175.57	6972.62	959.7403
	W14×159	301.2897	79083.97	7625.80	1052.1407
Beam Elements	W16×40	76.1289	21560.79	1926.86	268.3925
	W21×44	83.8708	35088.31	2122.81	338.4771
	W21×50	94.8385	40957.17	2400.41	391.8663
	W24×55	104.5159	56191.24	2645.35	475.1232
	W24×62	117.4191	64515.87	2971.94	541.6055

used in this actual study. The effective modal mass summed to the fifth mode is 95.4%, which means it has enough accuracy to perform the analysis. In the numerical analysis to determine the response to the input earthquake motion, a constant average acceleration method has been selected. For the damping of the objective structure, Rayleigh damping has been used as follows¹⁰⁾.

$$[C] = a_0 [M] + a_1 [K] \quad (1)$$

where, [C] = damping matrix; [M] = mass matrix; [K] = stiffness matrix; a₀, a₁ = constants

Table 3. Natural periods of each mode of the objective structure

Mode	Natural Period (sec)		Modal Participation Factor	Mass Participation Factor
	this Study	SAP2000N		
1	2.183	2.183	-17.647	0.733
2	0.810	0.810	-7.473	0.131
3	0.484	0.484	-4.473	0.047
4	0.334	0.334	3.330	0.026
5	0.250	0.250	-2.725	0.017
6	0.198	0.198	-2.055	0.010
7	0.160	0.160	1.803	0.008
8	0.148	0.148	0.000	0.000
9	0.137	0.137	-0.812	0.002
10	0.136	0.136	1.363	0.004

If the same damping ratio is given to adjacent two modes, a_0 and a_1 can be obtained by Eq. (2).

$$a_0 = \xi \frac{2\omega_i\omega_j}{\omega_i + \omega_j}; \quad a_1 = \xi \frac{2}{\omega_i + \omega_j} \quad (2)$$

where, ω_i and ω_j are the angular frequencies of i and j mode, respectively.

We assume that the damping ratio is 5% to get a_0 and a_1 from two periods of the first mode and the second mode. The Rayleigh modal damping matrix is obtained using Eq. (1) with values, $a_0 = 0.2099$ and $a_1 = 0.0094$. PGA according to each input earthquake motion increases from 0.1 g to 0.7 g with 0.1 g increments. Fig. 4 shows fourteen curved lines(7 solid & 7 dotted lines) of the maximum displacement on each story as PGA increases from 0.1 g to 0.7 g by 0.1 g increment. Solid lines represent the lateral joint displacement distribution of near-fault earthquakes, while dotted lines represent those of far-fault earthquakes. Fig. 4 shows that displacement increase rates of near-fault earthquakes are considerably larger than those of far-fault earthquakes. The lateral joint displacement of near-fault earthquake with PGA = 0.5 g exceeds that of far-fault earthquakes with PGA = 0.7 g.

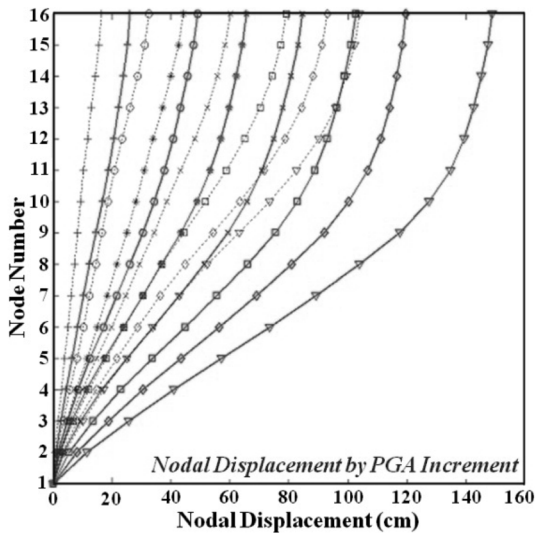


Fig. 4. Mean displacement responses with 0.1~0.7 g from left to right(solid lines : NFE PGA, dotted lines :FFE PGA)

Fig. 5 and Fig. 6 show the maximum inter-story drift on each floor with PGA = 0.1 g and 0.5 g. For a PGA of 0.1 g, an elastic behavior without plastic hinges occurs, and for a PGA of 0.5 g, an inelastic behavior with plastic hinges occurs for every input earthquake motion. In addition, the solid lines indicate near-fault earthquakes, and dotted lines far-fault earthquakes. Fig. 5 indicates that in an elastic state, the inter-story displacement of near-fault earthquakes on every floor is larger than that of far-fault earthquakes. It can be also seen that the maximum inter-story displacement occurs in the middle story of the structure. However, the inter-story drift distribution shown as in Fig. 6 is very different. Below the 10th floor, the effects of near-fault earthquakes are greater than that of far-fault earthquakes, but above the 10th floor, it is vice versa. In addition, the location of the maximum inter-story drift moves to lower stories. This result indicates that the response pattern to an input earthquake motion is very different according to the elastic/inelastic behavior of structure. If the structure has inelastic behavior and is affected by a near-fault earthquake, the inter-story drift occurs intensively in the lower stories, rather than in higher stories. In an elastic state, the effects of near-fault earthquakes are great on every floor. But in an inelastic state, the effects of far-fault earthquakes are

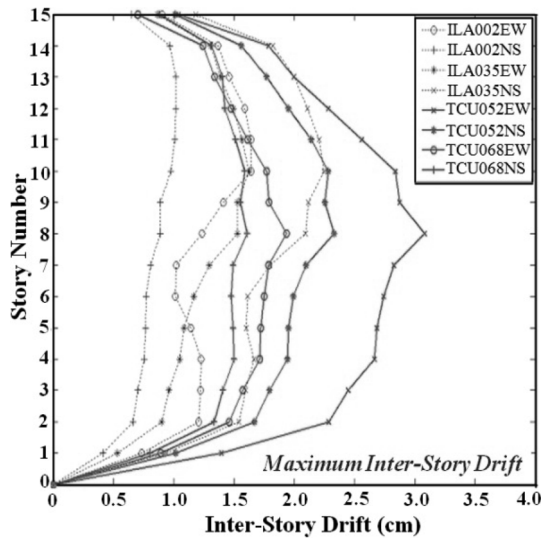


Fig. 5. Inter-story Drift Response with PGA = 0.1 g.

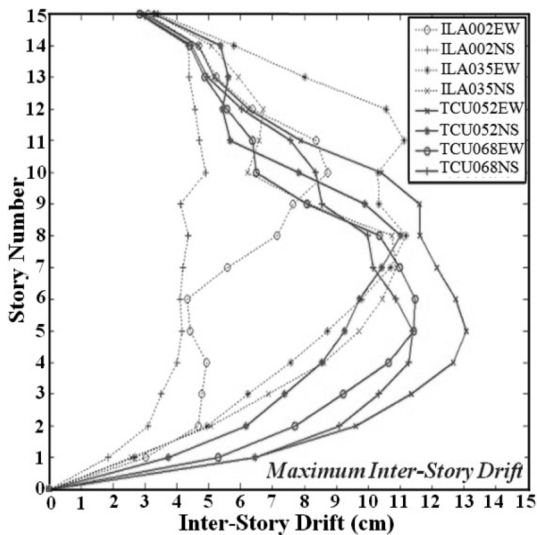


Fig. 6. Inter-story Drift Response with PGA = 0.5 g.

larger than those of near-fault earthquakes. This is because when pulses start, plastic hinges occurs intensively in the lower stories, while it does not affect the higher stories.

The Acceleration and displacement responses of roof story are compared by elastic and inelastic analysis when PGA = 0.5 g. Table 4 summarizes the maximum acceleration and displacement of earthquake characteristics by elastic and inelastic analysis. The mean acceleration and displacement responses of inelastic behavior are smaller than that of elastic behavior. In addition, the mean acceleration response of far-fault earthquakes is larger than that of near-fault earthquakes.

Table 4. Mean acceleration and displacement of near- and far-fault earthquakes by elastic/inelastic analysis

Site and Response	Maximum Roof Acceleration (gal)		Maximum Roof Displacement (cm)	
	Inelastic	Elastic	Inelastic	Elastic
ILA002EW	1311.84	2178.80	70.59	95.94
ILA002NS	1164.07	1695.20	50.63	71.89
ILA035EW	1189.57	1968.16	108.68	121.12
ILA035NS	1485.32	2817.80	86.55	168.79
Mean Value	1287.70	2164.99	79.11	114.44
TCU052EW	1178.19	1996.55	111.38	248.69
TCU052NS	1137.43	2021.97	91.95	189.55
TCU068EW	938.15	1344.54	99.86	154.07
TCU068NS	1161.94	2031.32	107.32	136.77
Mean Value	1103.93	1848.60	102.63	182.27

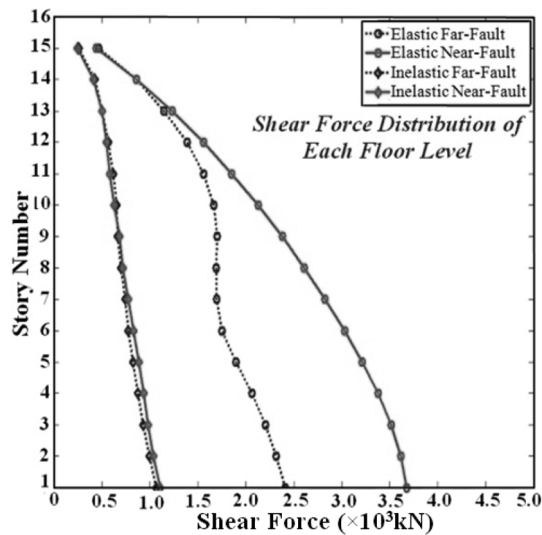


Fig. 7. Mean shear force distribution at each floor level by elastic/inelastic analysis.

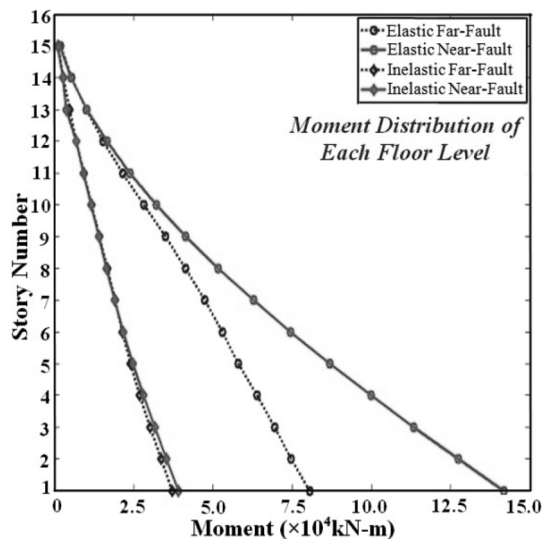


Fig. 8. Mean moment distribution at each floor level by elastic and inelastic analysis.

However, the mean displacement response is greater when it is influenced by near-fault earthquakes. Fig. 7 and Fig. 8 show the mean shear force and moment distribution of each story according to the characteristics of input earthquake motion. As shown in these figures, when in the elastic state and influenced by near-fault earthquakes, the shear force and moment of the lower stories is very high compared to those of the higher stories.

When the structures have inelastic behavior, the differences of shear force and moment between stories are reduced considerably. However, when the structures are affected by near-fault earthquakes, rather than by far-fault earthquakes, the difference is a little larger on the lower stories. Therefore, considering shear force and moment, we need to design bigger member sections to make it elastic. On the other hand, when we design it to have inelastic behavior, we can reduce the member section for a more economical situation.

2.3. Formating Process and Distribution of Plastic Hinges

Fig. 9 illustrates the fomulation process of plastic hinges under earthquake motion when $PGA = 0.7 g$. The plastic hinge which is newly formed is marked with solid circles, while the ones which already existed are marked with empty circles. The size of the circles is proportional to that of the plastic hinge. The creation of the plastic hinge is related the input earthquake motion and the duration of strong base motions. In the case of far-fault earthquakes, the duration of strong base motions is between 35 and 55 seconds. On the other hand the duration of strong base motions is between 33 and 40 seconds in the case of near-fault earthquakes, It can be seen that plastic hinges occur intensely in every member of the structure whose elastic limitation is surpassed when the big pulses appear. The size of the plastic hinge of near-fault earthquakes is bigger than that of far-fault earthquakes. In far-fault earthquakes, some

of the plastic hinge occurs in the high and low stories first, and then they gradually and more intensely move to the middle stories. Compared to far-fault earthquakes, the plastic hinge of near-fault earthquakes in the low stories are much bigger. Particularly in TCU068NS, the amount of plastic hinges in the low stories is much more than that of the middle stories. Therefore, we can conclude that the inelastic behavior of a structure under the influence of near-fault earthquakes depends on the size of the pulses and the duration.

3. Conclusions

According to the increase of PGA, the maximum displacement response on each story by near-fault earthquakes is larger than that by far-fault ones. The inter-story drift response has the maximum value in the middle story when the structure is in an elastic state. However, when the structure shows inelastic behavior, the inter-story drift has the largest value in the lower stories. In addition, the inter-story drift in an elastic state occurs greatly in every story. But when the structure has inelastic behavior, the lower stories are more influenced by near-fault earthquakes, while the higher stories are more affected by far-fault earthquakes. The shear force and moment distribution in each floor by elastic/inelastic time history analyses show that they get larger when the structure in an elastic state is more affected by near-fault earthquakes than by far-fault earthquakes. As the structure tends to inelastic behavior, the shear force

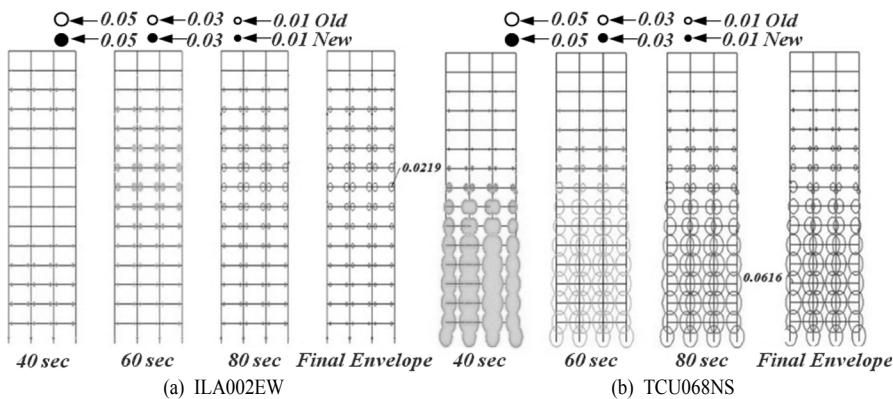


Fig. 9. Expansion process of plastic hinges for input earthquake motions (unit: rad).

and moment distribution become almost the same. From these results, it can be seen that long-period frame structures which are influenced by near-fault earthquakes will be economical if they are induced to have inelastic behavior. The formation process of plastic hinges influenced by near-fault earthquakes show big pulses, unlike those influenced by far-fault earthquakes. At this moment, the inelastic behavior of the structure is huge, and it can be seen that by the time the pulses are over, the inelastic behavior of the structure is also nearly over. In the case of far-fault earthquakes, the plastic hinge occurs first in the higher and lower stories, and then spread to the middle stories, where the biggest plastic hinge occurs. On the other hand, in the case of near-fault earthquakes, when the big pulses appear, the big plastic hinge occur in the lower and middle stories, and when the pulses are over, the inelastic behavior is complete. From the results above, it can be seen that long-period frame structures which are affected by near-fault earthquakes have different response patterns from those influenced by far-fault earthquakes. Therefore, when designing long-period structures which are located near to faults, it should be considered mandatorily in the design that the characteristics of near-fault earthquakes are reflected.

Acknowledge : The Research was supported by a grant from the Academic Research Program of Chungju National University in 2011.

References

- 1) M. S. Bang and S. H. Han, "A Study on Characteristics and Dynamic Response Spectrum of Near Fault Ground Motions", Journal of KOSOS, Vol. 20, No. 3, pp. 143~151, 2005.
- 2) G. W. Housner and D. E. Hudson, "The Port Hueneme Earthquake of March 18, 1957", Bulletin of the Seismological Society of America, Vol. 48, No. 2, pp. 163~168, 1985.
- 3) P. C. Jennings, "Enduring Lessons and Opportunities Lost from the San Fernando Earthquake of February 9, 1971", Earthquake Spectra, Vol. 13, No. 1, pp. 25~53, 1997.
- 4) B. A. Bolt, "Discussions of Enduring Lessons and Opportunities Lost from the San Fernando Earthquake of February 9, 1971", Earthquake Spectra, Vol. 13, No. 3, pp. 545~547, 1997.
- 5) Korea Atomic Energy Research Institute (KAERI) (2003). "Characteristics of Near-Fault Ground Motions", Report ID KAERI/TR-2453, 2003.
- 6) G. Q. Wang, X. Y. Zhou, Z. J. Ma and P. Z. Zhang, "Corrected Near Fault Recordings Caused by the 1999 Chi-Chi, Taiwan Earthquake", Bulletin of the Seismological Society of America, Vol. 9, No. 5, pp. 1358~1369, 2001.
- 7) UBC Code (1991-1997), "Uniform Building Code, International Conference of Building Officials (ICBO)", Whittier, CA.
- 8) Building Seismic Safety Council "NEHRP recommended provisions for the development of seismic regulations for buildings", FEMA-222, Washington, D C., 1994.
- 9) SAP2000 Analysis reference Volume I, II, Computer and Structures Inc., 1997.
- 10) K. Chopra, "Dynamics of Structures: Theory and Applications to Earthquake Engineering", Prentice Hall, Inc., 1995.